Proceedings IRF2018: 6th International Conference Integrity-Reliability-Failure
Lisbon/Portugal 22-26 July 2018. Editors J.F. Silva Gomes and S.A. Meguid
Publ. INEGI/FEUP (2018); ISBN: 978-989-20-8313-1

PAPER REF: 7223

NUMERICAL AND EXPERIMENTAL ANALYSIS OF AERONAUTICAL CFRP COMPONENTS SUBJECTED TO STRUCTURAL LOADS

A. Castriota, V. Dattoma, R. Nobile, F.W. Panella(*), A. Pirinu, A. Saponaro
Department of Engineering for Innovation, University of Salento, Lecce, Italy
(*)*Email:* francesco.panella@unisalento.it

ABSTRACT

In this work, numerical models and experimental tests are performed to validate analysis methods applied on aeronautical CFRP components. In particular, tests of a multi-stingers panel under static compression load and a repaired spar under dynamic bending load are reported. The FEM model are realized to reproduce the panel's geometry and stacking sequence, the constraints and representative loads of the component's service. Numerical models are improved to reduce the differences between the calculated and experimental deformations, allowing the experimental test validation. In the multi-stringer panel, the experiences evaluate the effects of the out-plane deformations due to compression failure, the difficulties of alignment and distribution's load along and finally the validation of the numerical model. While in the spar's study, the experimental measurements confirmed the predictions of the numerical model.

Keywords: bending test, buckling, CFRP, compression test, numerical model, multi-stringers panel, spar.

INTRODUCTION

Numerical and experimental tools are generally used to evaluate the structural behavior of aeronautical CFRP components. Each tool introduces specific approximation and hypothesis to derive information about stiffness, durability and mechanical strength of structural elements before the possibility to use it in aeronautical structures.

Numerical models are generally based on ideal geometrical configuration, ideal material behavior and simplified constraints and loads. On the other hand, experimental tests are affected by discrepancies between nominal and effective geometry of the test article and introduce errors due to an uncorrected application of constraints and loads. As a result, the structural behavior of a real component could be considered known with an acceptable reliability level only if both numerical and experimental tools are used.

In this work, the mechanical behavior of two CFRP aeronautical structural elements has been studied both from a numerical and experimental point of view. The result of numerical analysis has been used to give useful indications in order to define the experimental test procedure.

Static analysis allows performing the experimental setup and avoiding eccentric loads that could cause component failure at lower critical load or other incorrect results.

MATERIALS AND COMPONENTS' GEOMETRY

The first test article that has been studied is an aeronautical multi-stringer component of medium size (914.4 x 762 mm^2) in carbon fibre laminates (Figure 1). All laminates are CFRP laminates with different ply layers. In this component, rivets secure the ribs on the skin. The component presents an artificial discontinuity in the form of a large cut (152.4 x 6.35 mm^2) with extremities. This artificial damage on the skin interrupts the central stringer and simulates the presence of impact damage on the stringers area (Figure 1b).

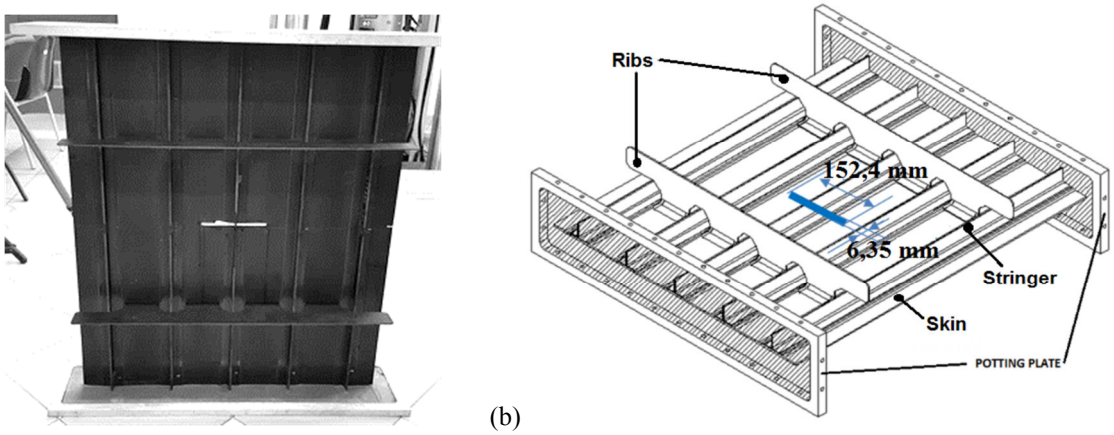

(a) (b)

Fig. 1 - CFRP multi-stringer component's geometry (a) and artificial damage's geometry (b).

The laminae are constituted by CFRP fabric with a texture such that the major mechanical characteristics are those that are detected in the warp direction parallel. The information in terms of material and lamina properties constituents are shown in Table 1.

Table 1 - Properties of composite parts of multi-stringer component.

Part component	Sub-Part component	Material	Lamina Thickness [mm]	N° plies	layup
Skin	Skin Thin	IMS/977-2	0.186	20	$[45/90/-45/-45/45/90/0/-45/45/0]_S$
	Skin Big	IMS/977-2	0,186	24	$[45/90/0/0/-45/-45/45/90/0/-45/45/0]_S$
Stringer		IMS/977-2	0.186	12	$[45/90/0/0/-45/0]_S$
Rib		HTA/977-2	0.208	12	$[45/0/-45/90/45/0]_S$

The second component is a spar (1044 mm length) with a double-T section in composite material having upper and lower skins co-cured thereon and represents the rear spar of a horizontal stabilizer of an aircraft. The spar material is CFRP composite constituted of two parts, the skin and the web (Figure 2). The web part is built with 20 plies (lamina thickness of 0.178 mm) and total thickness of 3.56 mm. The skin part is realized with 10 plies (lamina thickness of 0.178 mm) and 50 additional plies (lamina thickness of 0.172 mm) for a total thickness of 10.4 mm.

The structure presents on the core a hole of about 10 cm in diameter on whose edge a scarfing and hot bond technique is provided to restore the structural integrity of the part. This technique is based on the application of a certain number of sub-laminates (called patches) polymerized and subsequently superimposed on the part to be repaired, interposing layers of

adhesive. In this way it is possible to make the sub-laminates adhere perfectly to the component profile without giving rise to high internal stresses. In the case of composite materials, unlike metals, they are applied with bevel joining techniques, minimizing the increase in thickness and allowing a uniform distribution of shear stress in the adhesive. Figure 2 shows the component's geometry and its parts.

(a) (b)

Fig. 2 - CFRP aeronautical spar's geometry (a) and component's geometry (b).

This structural component is equipped with aluminium supports (employing to support the spar during the loading phase). The information in terms of material and lamina properties constituents are shown in Table 2.

Table 2 - Properties of composite parts of aeronautical spar.

Part component	Sub-Part component	Material	Lamina Thickness [mm]	N° plies
Skin	Skin Thin	IMS/977-2	0.178	10
	Skin Big	IMS/977-2	0.172	50
Web		IMS/977-2	0.178	10

EXPERIMENTAL SETUP AND METHODS

The execution of the experimental tests on this aeronautical components involves the use of a machine capable of exerting very large forces, safely, to bring the multi-stringer component to the crisis due to instability of equilibrium. The experimental campaign was conducted at the EMILIA laboratory of Università del Salento using a base frame and two large cubic structures to constraint the components and a hydraulic actuator driven by a closed loop controller to apply the load.

The base (Figure 3a) is essentially a grid of beams with plan dimensions of 5m x 9m, consisting of beams of the HEB 300 series provided with holes for fixing the accessories to perform mechanical tests. Two modular test benches (2x2 m^2 and height 1.2m) are used to hold the test article and the actuator. The cubic benches are obtained by assembling five steel plates of appropriate size that have a thickness of 150 mm; the benches are equipped with inverted T-slots on each face specially designed for attaching specimens, accessories and actuators.

In these specific tests, the load application is obtained through MTS 244 series hydraulic actuators (Figure 3b), that develop a maximum force of 500 kN (in traction and compression) and a stroke of 500 mm. The actuator is equipped with a load cell such that it is possible to

perform both displacement and force control tests. Digital controller is a MTS Flextest100 having the possibility to control up to 8 actuators.

In Figure 4a there is a demonstration configuration of the structure on which the two large components have been fixed to be tested simultaneously, while the Figure 4b shows the test control area in the laboratory EMILIA. Figure 5 shows the laboratory EMILIA with test setup of two components.

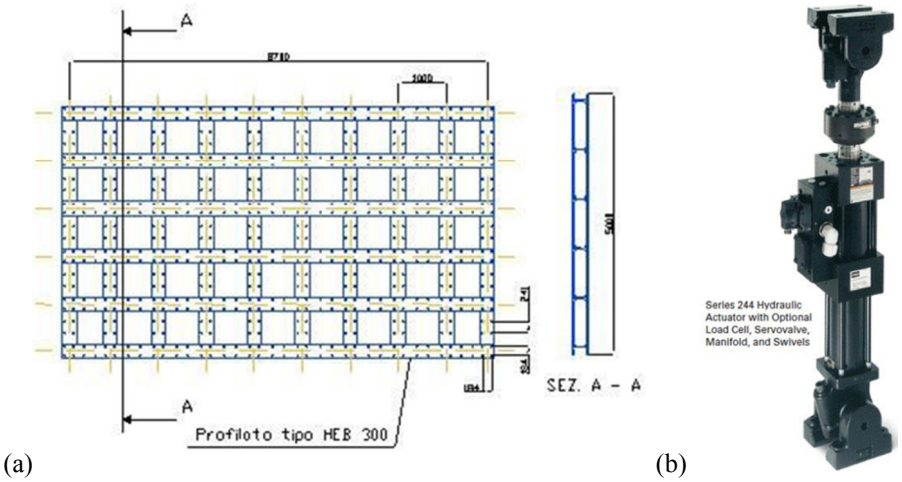

(a) (b)

Fig. 3 - Base frame's geometry (a) and MTS Hydraulic Actuator (b).

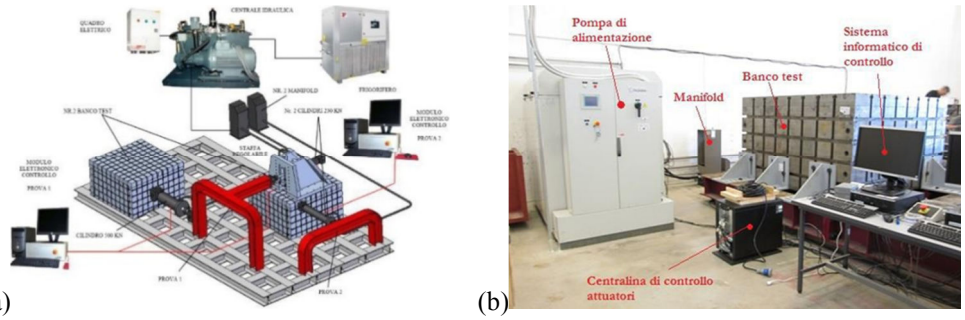

(a) (b)

Fig. 4 -Test facility configuration (a) and test control area of laboratory (b).

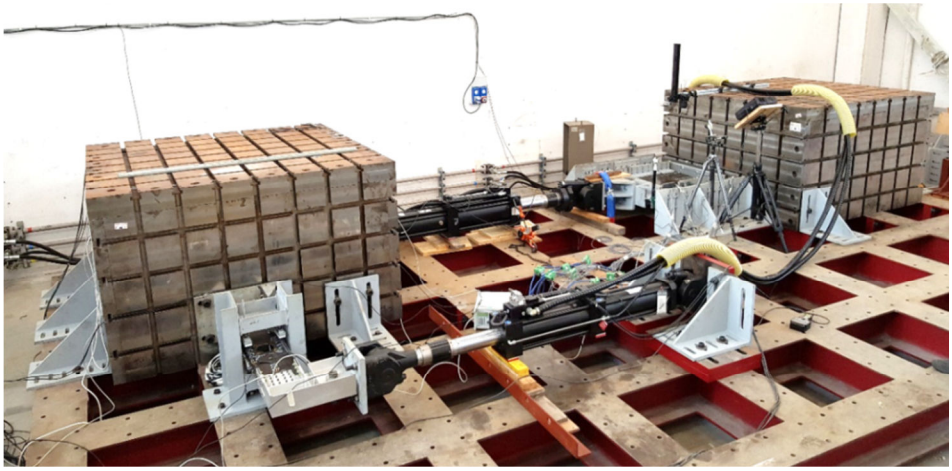

Fig. 5 - Experimental setup in the Laboratory EMILIA.

The assembly of the several components on the test machine requires the presence of dedicated structures allowing replicating, as closely as possible, the constraint conditions that exist on the actual multi-stringer component and reproducing the geometric and structural continuity of the surrounding structure.

For the specific test multi-stringer component, anti-buckling guides have been used on the side edges to reproduce the continuity of material that would exist in the original structure. In this way, the local instability of the multi-stringer component near the notch is highlighted. These guides are coated in Teflon to prevent the surface of the multi-stringer component encounters some type of resistance during the loading phase.

In Figure 6a, the anti-buckling guides are placed both below and above the multi-stringer component. Figure 6b shows the positioning of the multi-stringer component on the guides.

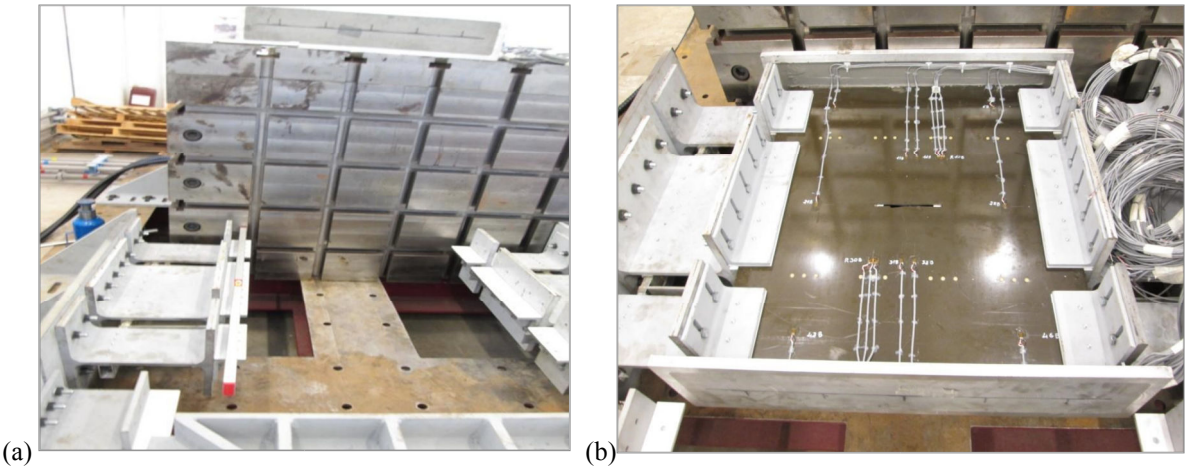

(a) (b)

Fig. 6 - Alignment of supporting multi-stringer component guides (a) and positioning of the multi-stringer component on the guides (b).

The spar will be subjected to a fatigue load; the tests are performed to predict the static and dynamic behaviour of a composite repaired spar representative of an aeronautical stabilizer (Megson, 1999). In this work, a static preliminary test is carried out in order to verify the correct application of load and constraints to the test article.

The spar is fixed at one extremity and transversally pin-loaded at the other extremity obtaining a bending load. A rigid metallic structure is used to avoid local buckling phenomena at the spar middle length (Figure 7).

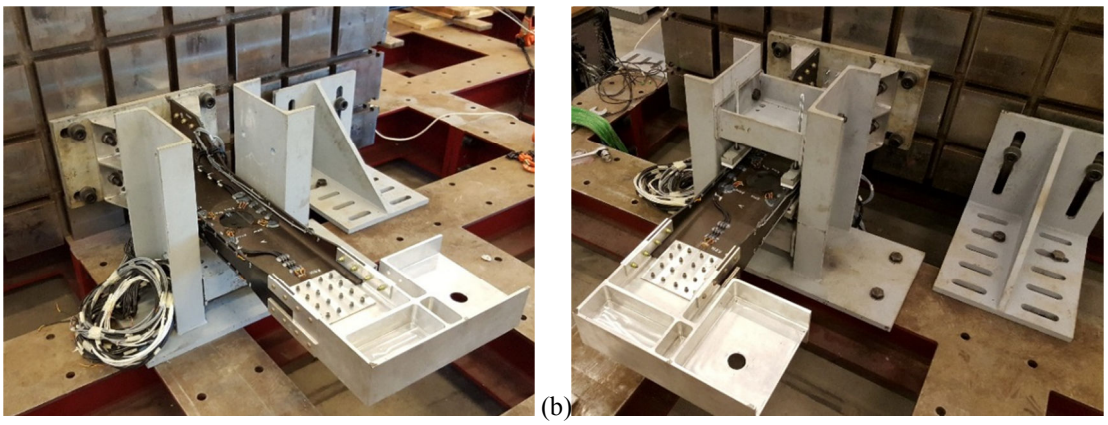

(a) (b)

Fig. 7 - Spar positioning on cubic benches structure (a) and anti-buckling structural setup (b).

The arrangement of some strain gauges and rosettes in selected points of the two-test article allows the verification of the correct application of the load and the evaluation of the resulting strain state, which can be compared to the numerical one.

The multi-stringer component has been equipped with 80 strain gauges, in order to monitor the test and to check the load the alignment. The Figures 8 and 9 show views and maps of the multi-stringer component fully instrumented and ready for the tests.

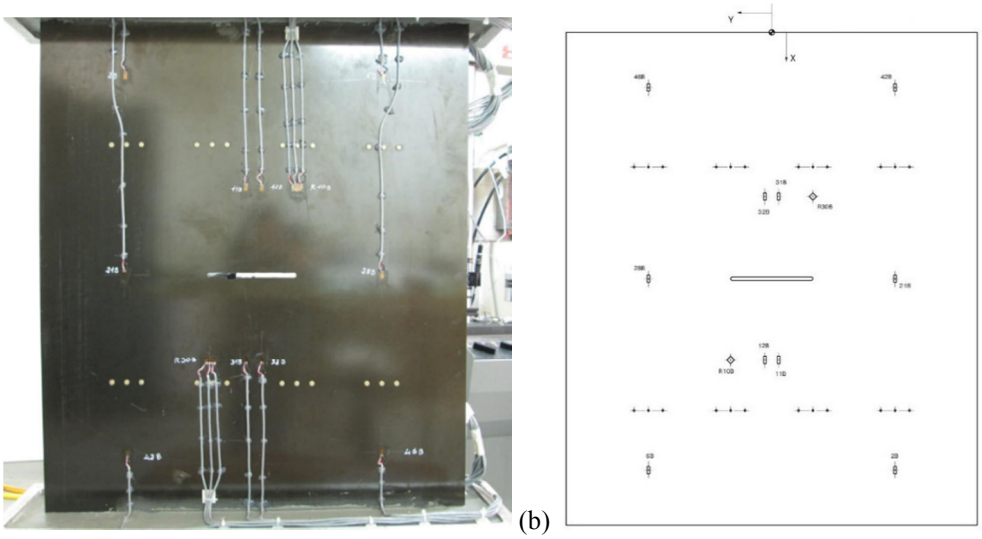

(a) (b)

Fig. 8 - Front view (a) and strain gauges map (b) of fully instrumented multi-stringer component.

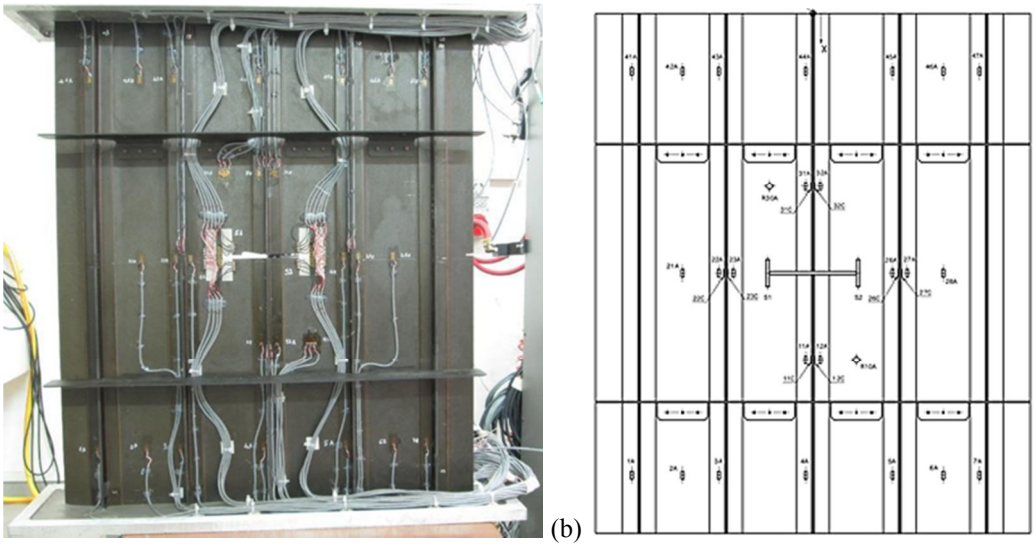

(a) (b)

Fig. 9 - Back view (a) and strain gauges map (b) of fully instrumented multi-stringer component.

Starting from the same consideration, the spar component has been equipped with 32 strain gauges and 10 rosettes (with grids at 0 ° / 45 ° / 90 °), as illustrated in Figure 10.

The Figure 11 shows the final layout used for the compression test on the CFRP multi-stringer component and for the static load test on CFRP aeronautical spar. These preliminary static tests were carried out with compression load of 50 kN on the multi-stringer component and of tension-compression load of 5 kN on the spar, in prevision of future buckling analysis on multi-stringer and fatigue study on the spar.

(a) 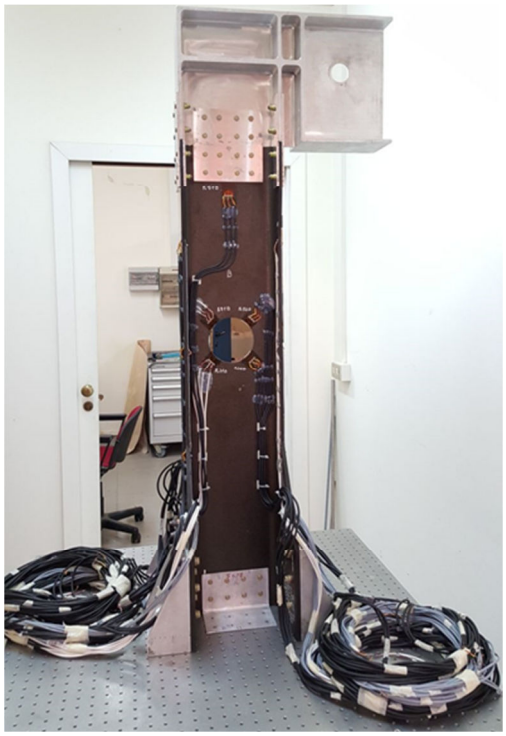 (b) 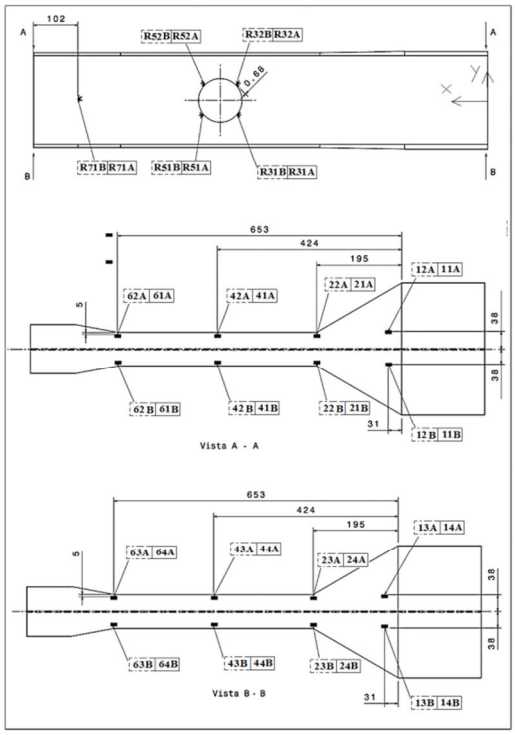

Fig. 10 - Front view (a) and strain gauges map (b) of fully instrumented aeronautical spar.

(a) 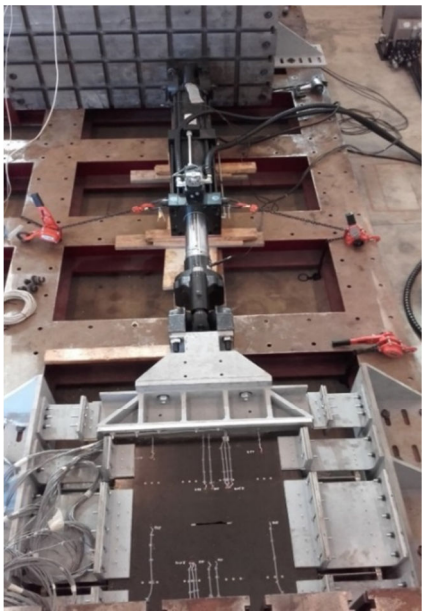 (b) 

Fig. 11 - Final layout of the multi-stringer component compression test (a) and of static spar test with the anti-buckling structure (b).

FINITE ELEMENT ANALYSIS

Numerical analysis of components was carried out with ANSYS 16.2 Mechanical APDL; in some work phases, Matlab was also used. The modelling of completely multi-stringer component was carried out (Figure 12) to evaluate deformation of different points of both skin and stringers after the buckling analysis, because equilibrium instability not necessary involves a symmetrical deformed configuration.

The main material of the multi-stringer component is the laminate CFRP, with oriented appropriately different laminae to achieve the required strength and stiffness, while the rivets are made of titanium alloy. The rivet is modelled with a Beam188 element and the skin, ribs and stringer with Shell281 element. The local buckling phenomenon is then analysed, identifying the first critical load causes the multi-stringer component failure and studying the deformation modes. The deformation analysis was carried out applying a compression load of 50 kN. In the following Figures 13 and 14, the deformation maps along the load axis (X-axis) and normal load plane (Z-axis) are shown.

The damage in aeronautical structures can reduce mechanical strength and stiffness of the components' material (Mallick, 1993). In particular, the compressive stresses can lead to a state of instability of the condition buckling in the structure itself (Singer *et al*., 2002).

Therefore, a linear elastic buckling analysis was carried out. The displacement map of the multi-stringer component subjected to equilibrium instability, shows that the constraints' application reproduces buckling phenomenon localization, with an evident leaking of the original plane skin (Figure 15a).

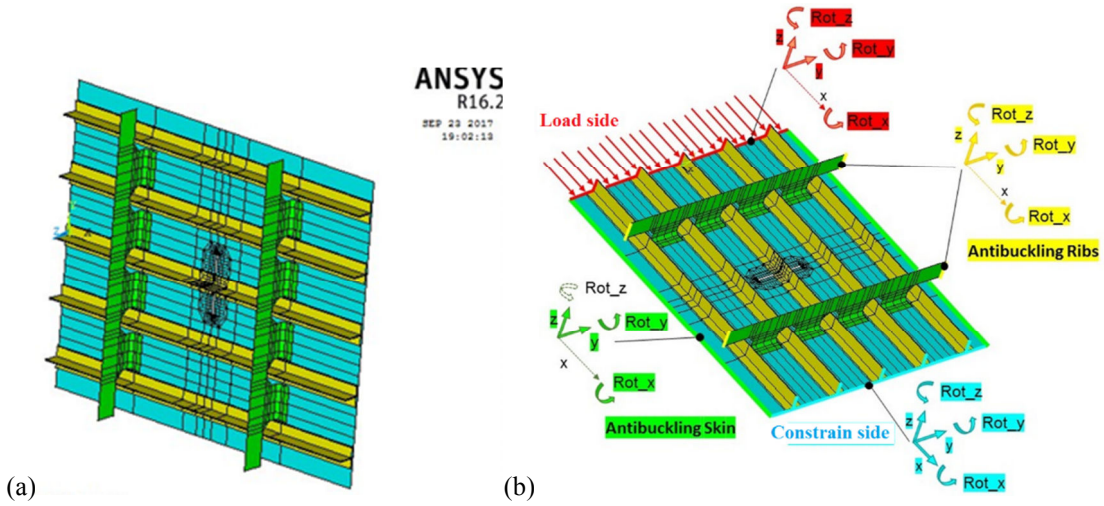

Fig. 12 - Front view of model's geometry (a) and modelling with applied constrains and loads (b).

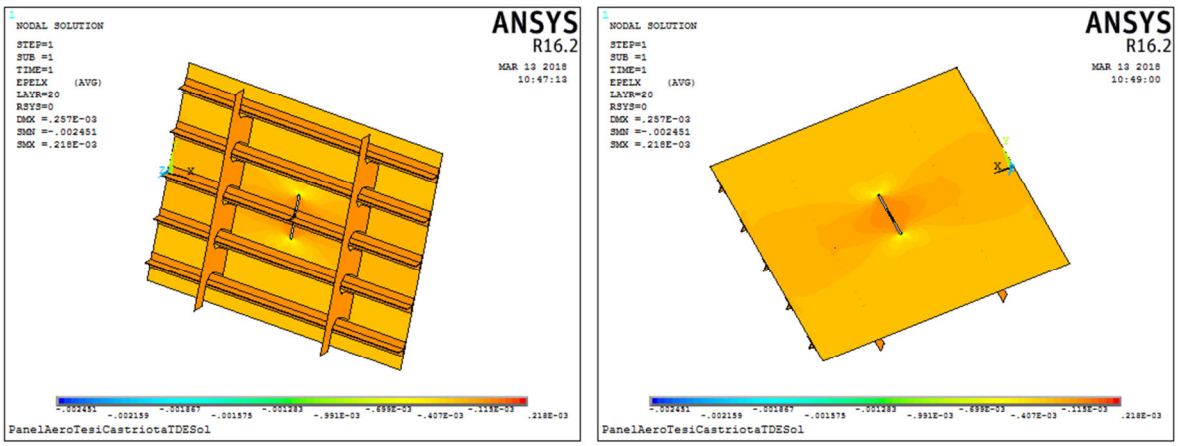

Fig. 13 - Deformation maps along X (longitudinal) direction for test load of 50 kN.

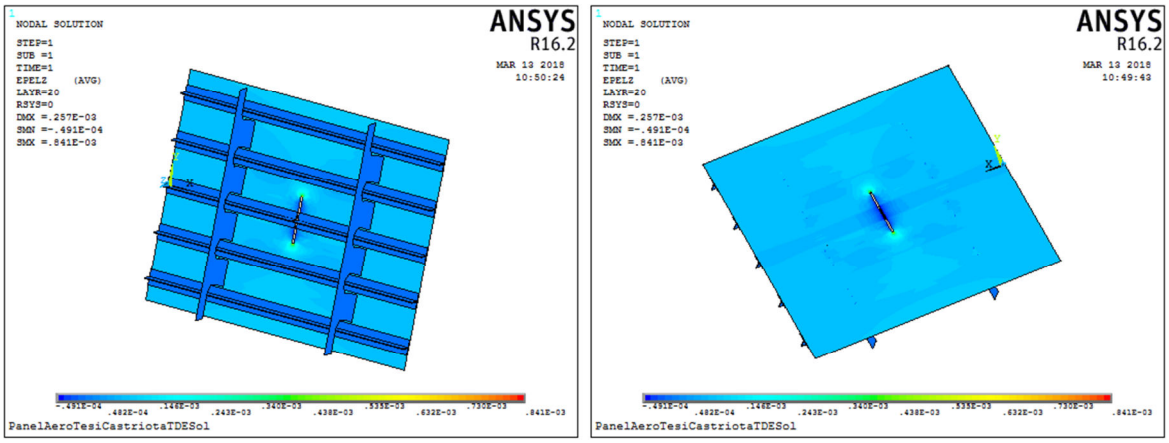

Fig. 14 - Deformation maps along Z (normal load plane) direction for test load of 50 kN.

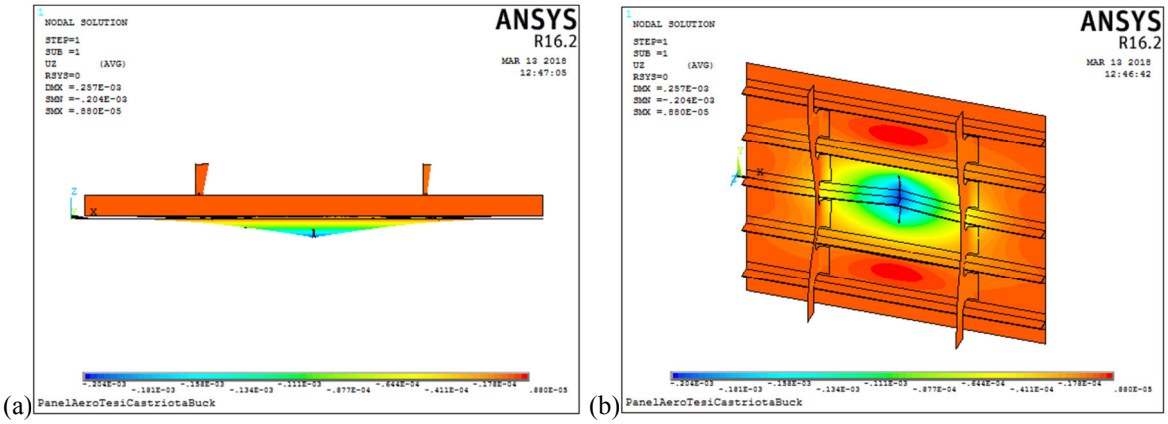

Fig. 15 -Side view of the displacement map (a) and orthogonal view of displacement map in the multi-stringer component's plane (b).

The second numerical model was realized to predict the static and dynamic behaviour of the spar representative of an aeronautical stabilizer (Megson, 1999). The spar repair is neglected for the numerical model, which is not relevant in order to determine the global behaviour of the test article. Numerical model is built with Shell281 elements (Figure 16). The static analysis is realized applying loads and constrains on the numerical model to simulate the real bending load condition during the life service.

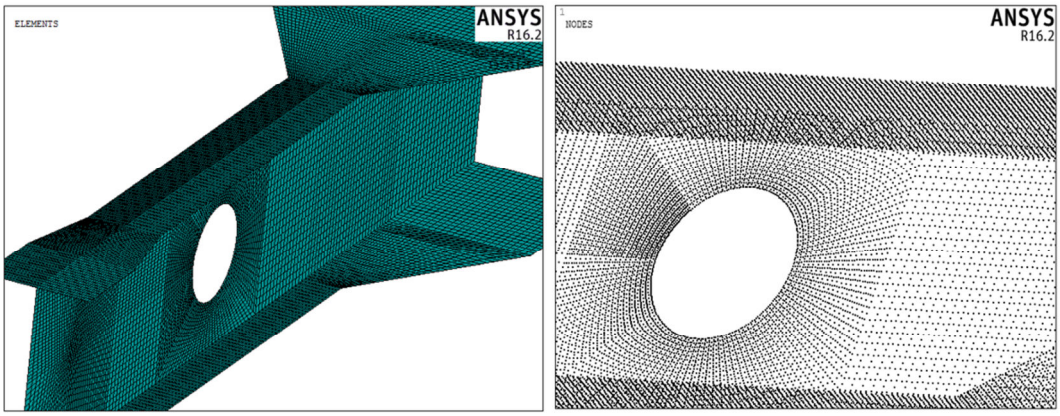

Fig. 16 - Numerical discretization modelling of CFRP spar.

The deformation analysis was carried out with a bending static load of 5 kN (Figure 17a). After the general postprocessor and the evaluation results FEM analysis, these results are compared with experimental data. The spar model is inflected and deformed into XY deflection plane.

We observed that the most stressed nodes are always near the hole zone and into the section variation area. Figure 18 represents the deformations contour plot along X in and along Y (load direction) axes.

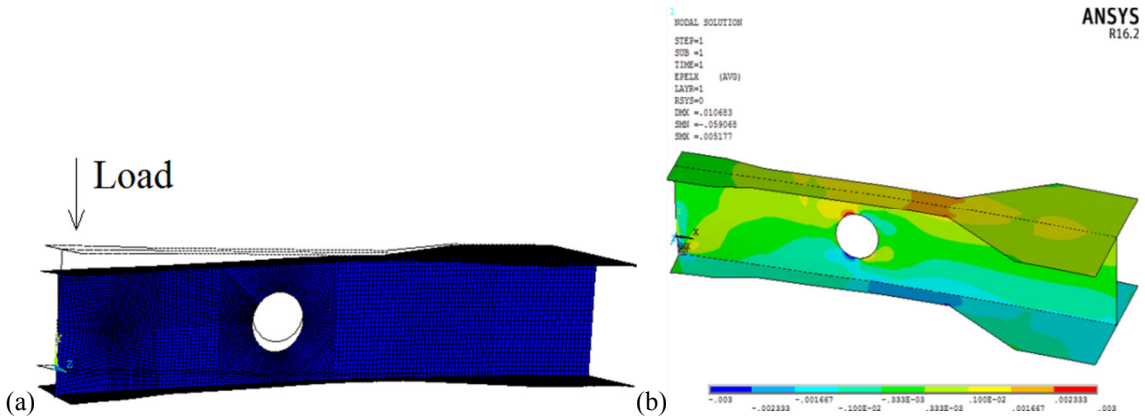

Fig. 17 - Deformed spar geometry along Y-axis of load application

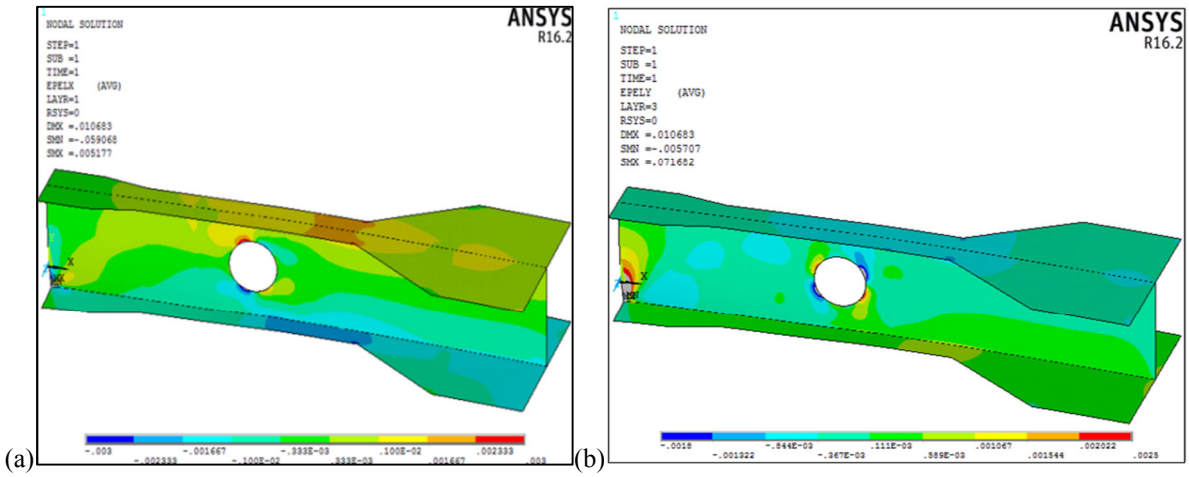

Fig. 18 - Deformation maps along X-axis direction (a) and Y-axis of load application (b).

EXPERIMENTAL RESULTS AND DISCUSSION

The post-processing allows interpreting and evaluates the experimental and numerical procedure in these test cases of aeronautical components. The result shows differences in the values of the deformations calculated by the numerical model and the measured deformations.

These results depend on the real transmission mode of loads from the actuator to the composite, on the conditions of blocking the opposite side to the load side and from the effect produced by specific anti-buckling guides.

Multi-stringer panel was subjected to a static compressive load up to 50 kN in load control. During the loading phase, strain measurements are recorded obtaining the behaviour reported in Figure 19. The strain behaviour recorded at the different locations allows verifying the correct application of the load and the uniformity of the applied stress state. The test configuration was therefore verified and suitable for the execution of the destructive test in a second moment.

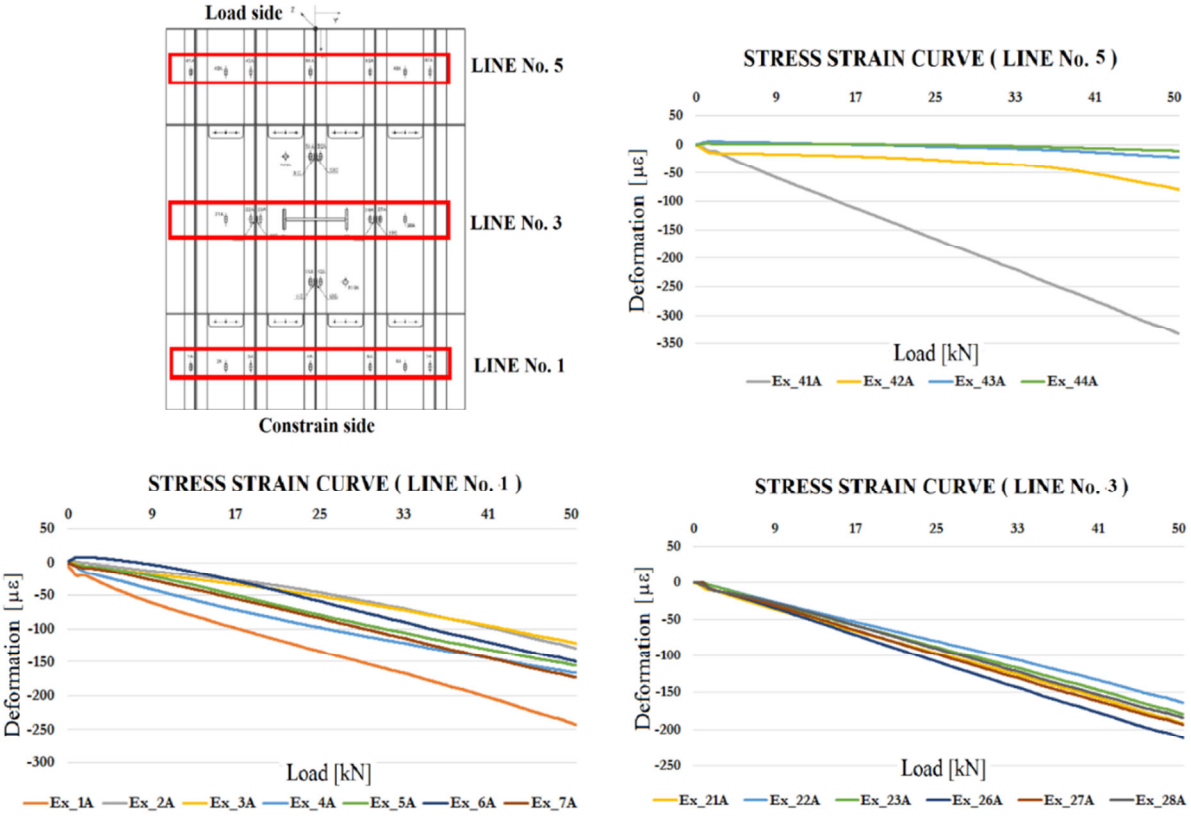

Fig. 19 - Deformation load curves at different location on back side of multi-stringer component.

Aeronautical spar was loaded up to 5 kN in load control in both direction in order to verify the correct application of the load prior to start the fatigue test. The measured strains are reported in Figure 20 and are coherent with the predicted one.

CONCLUSIONS

The mechanical behavior of two aeronautical components was evaluated using numerical models and experimental test. Numerical models have been realized in order to predict the strain distribution and used as reference for the subsequent experimental tests. These results allowed the improvement of the numerical model in order to reduce the differences between calculated and measured deformations, in order to allow the validation of the same through the use of experimental tests.

From the comparison, the experimental measurements were found in good agreement with the predictions of the numerical model, highlighting on the one hand the reliability of the modeling to the finite elements and on the other hand the accuracy of the experimental measurements.

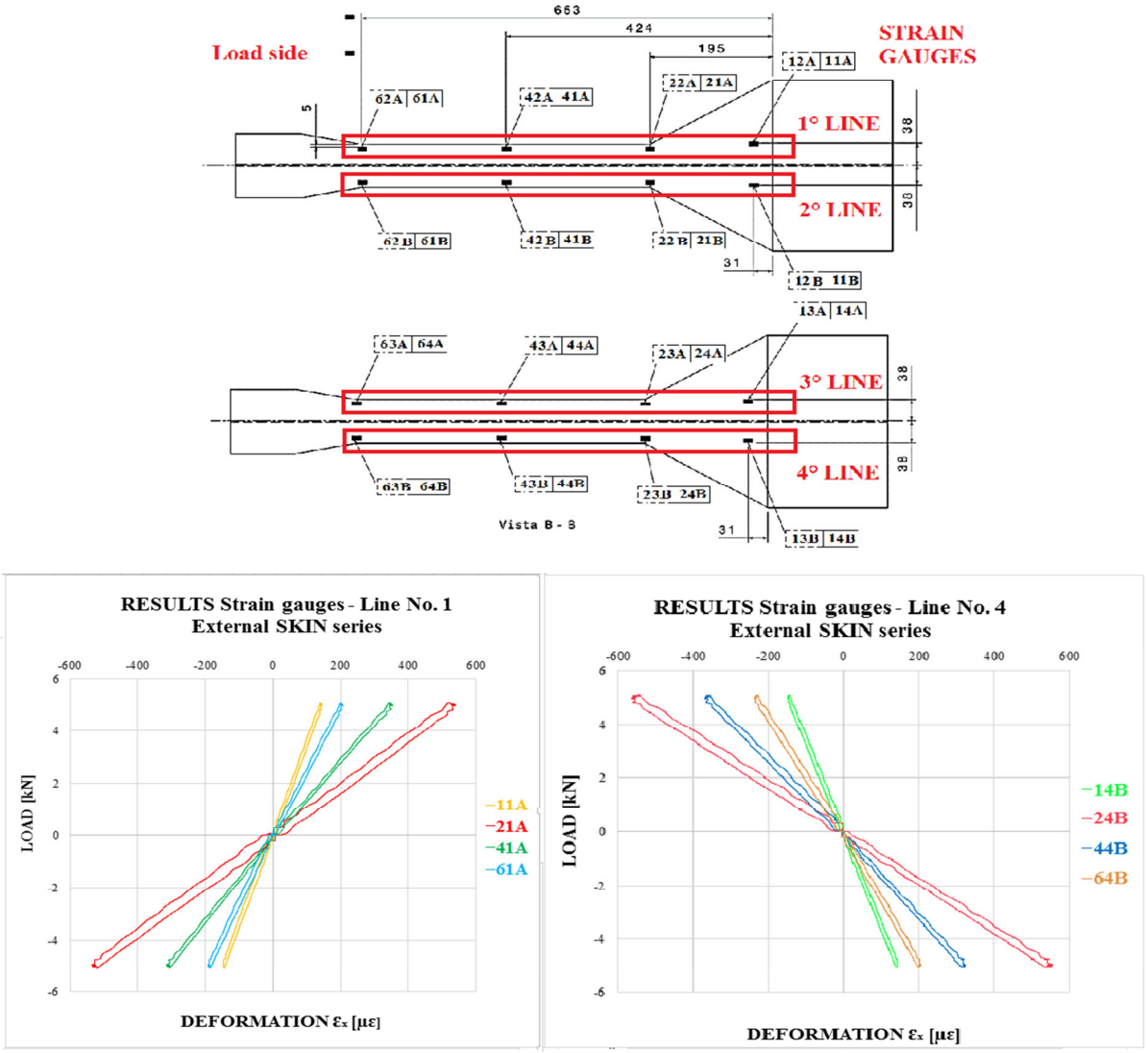

Fig. 20 - Deformation load curves at different location on skin part of spar.

REFERENCES

[1] T. H. G. Megson, Aircraft structures for engineering students, Elsevier, 1999, Amsterdam.

[2] P. K. Mallick, Fiber-reinforced composites: materials, manufacturing and design, Dekker, 1993, New York.

[3] R. M. Jones, Mechanics of composite materials, Taylor & Francis, 1975.

[4] J. Singer, J. Arbocz e T. Weller, Buckling Experiments, John Wiley & Sons Inc., 2002, New York.